Supporting Information

Sensitivity determination of energetic materials from laser spark spectrometry based on physical parameters corrected statistically methods

Xianshuang Wang[a], Junfeng Wang[b], Ying Fu[c], Ruibin Liu[a,*], Yage He[a], An Li[a], Denan Kong[a], Wei Guo[a], Qinghai Shu[b,*], and Yugui Yao[a,d,*]

[a]Key Lab of advanced optoelectronic quantum architecture and measurement (Ministry of Education), Beijing Key Lab of Nanophotonics & Ultrafine Optoelectronic Systems, School of Physics, Beijing Institute of Technology, Beijing 100081, China.
[b]School of Materials Science and Engineering, Beijing Institute of Technology, Beijing 100081, China. [c]School of Computer Science and Technology, Beijing Institute of Technology, Beijing 100081, China. [d]Frontiers Science Center for High Energy Material (MOE), Beijing Institute of Technology, Beijing 100081, China.

* Correspondence author:
TEL: +86-13520398457. E-mail: liusir@bit.edu.cn (Ruibin Liu)
TEL: +86-010-68915072. E-mail: qhshu121@bit.edu.cn (Qinghai Shu)
TEL: 86-010-68918672. E-mail: ygyao@bit.edu.cn (Yugui Yao)

Contents

Supplementary texts

Typical LIPS spectra.

The main characteristic peaks including C (193.1 nm, 247.9 nm), H (656.3 nm), N (742.4 nm, 744.2 nm, 746.8 nm, 868 nm, 870.3 nm, 871.2 nm), O (unresolved triplet at 777.2 nm, 777.4 nm, 777.5 nm) as well as CN bands (358.7 nm, 388.2 nm) and weak C2 band (516.5 nm) are involved. Peaks of some impurities, such as calcium and sodium are also observed. The emission from ambient argon is basically in the infrared band. All above elements are matched according to Atomic Spectra Database (ASD) of National Institute of Standards and Technology (NIST, see https://physics.nist.gov/PhysRefData/ASD/lines_form.html).

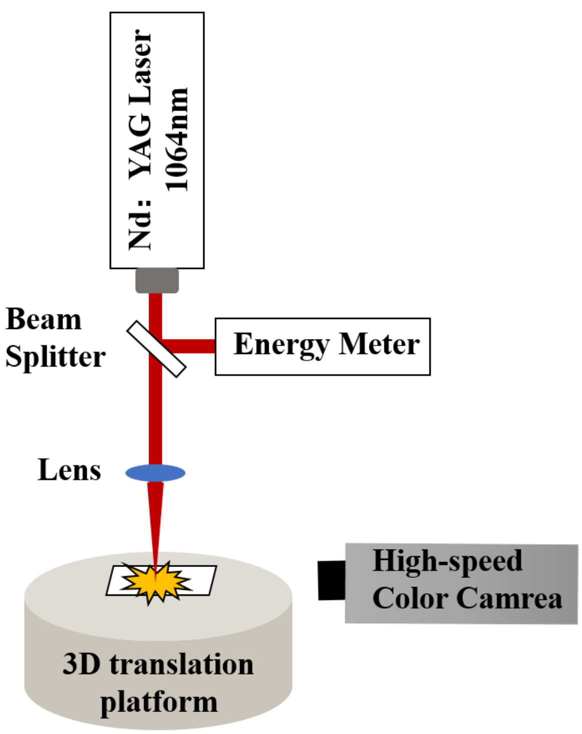

Supplementary Figure 1. Experimental setup for laser sensitiveness test of EMs.

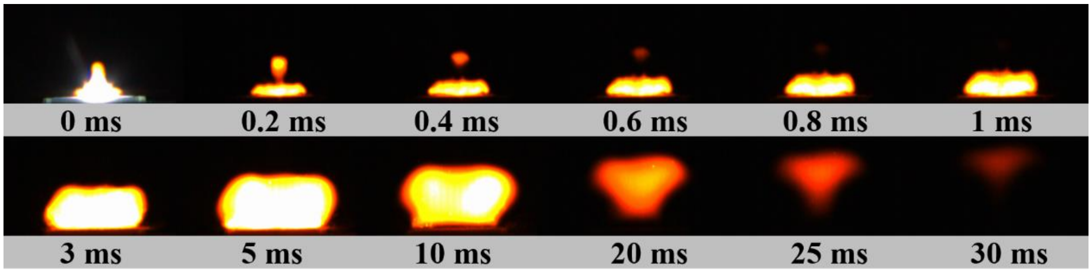

Supplementary Figure 2. The dynamic laser-produced deflagration of sample D1.

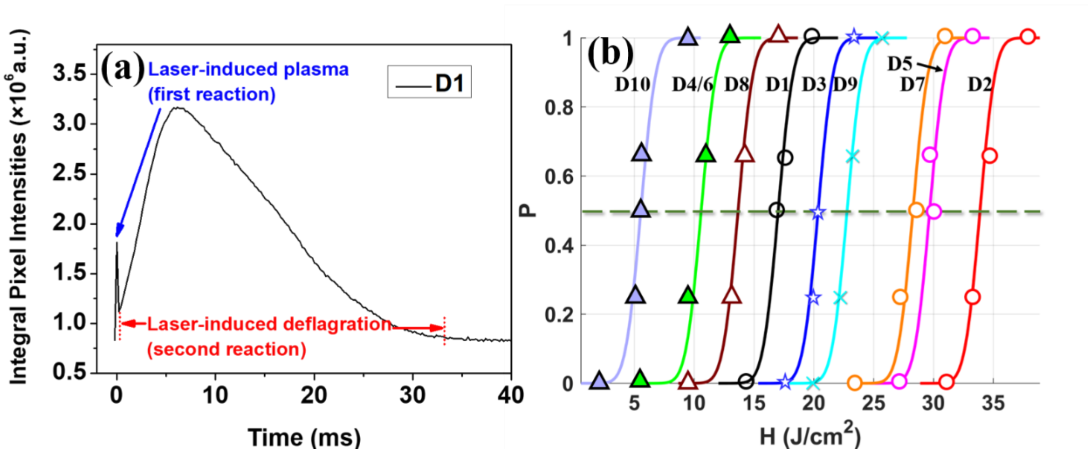

Supplementary Figure 3. Laser ignitibility. a Integral pixel intensities from time-dependent snapshots of laser-induced deflagration under the laser fluence of 70 J/cm^2 for sample D1. b Dependence of the probability of ignition (P) on the energy density of laser radiation (H) for single-compound explosives. Points show the experimental data and curves are their approximations.

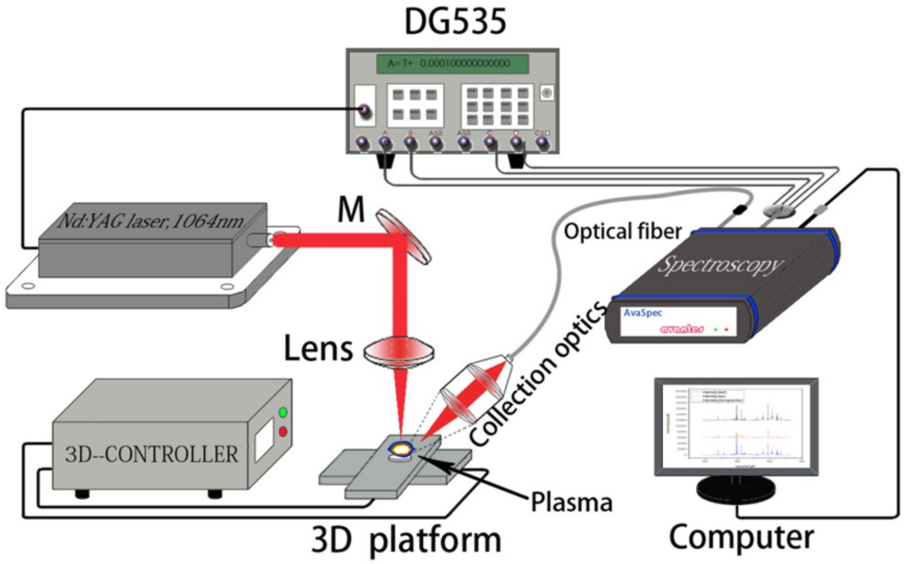

Supplementary Figure 4. LSS System.

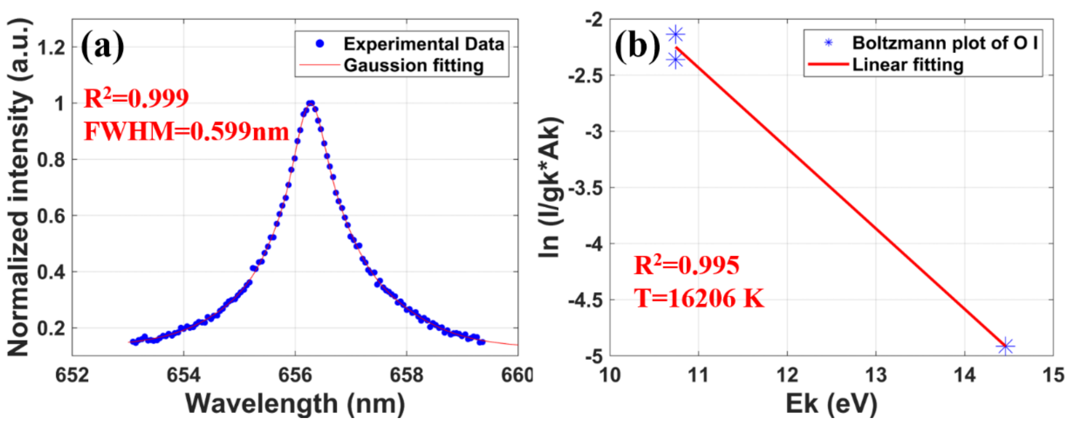

Supplementary Figure 5. Calculation of plasma parameters. (a) Gaussian fitting of Hα and (b) Boltzmann plot of O. R^2 represents goodness of fit.

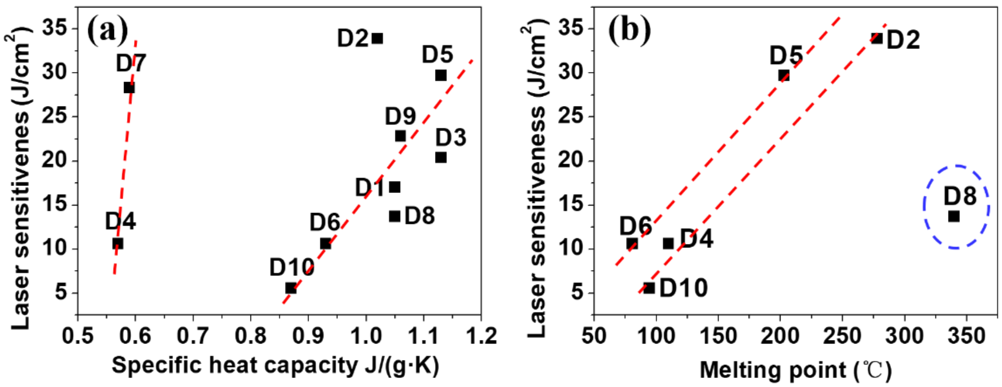

Supplementary Figure 6. The correlation between laser sensitiveness and specific heat capacity (a) and melting point (b). Red dash line marks the linear trend. (Note that sample D1, D3, D7 and D9 has no melting point and sample D8 is an outlier).

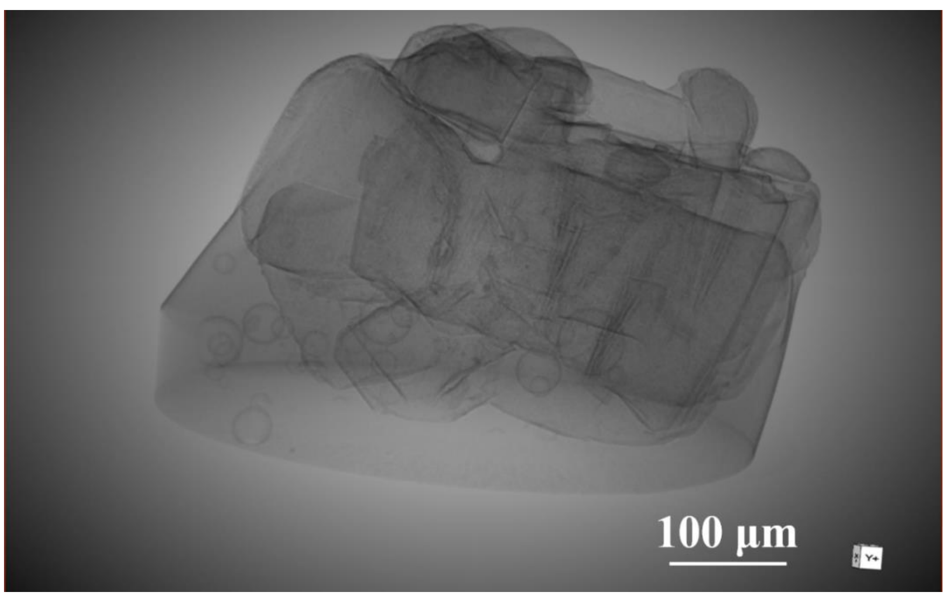

Supplementary Figure 7. 3D reconstructed figure of a NTO single particle by X ray microscopy.

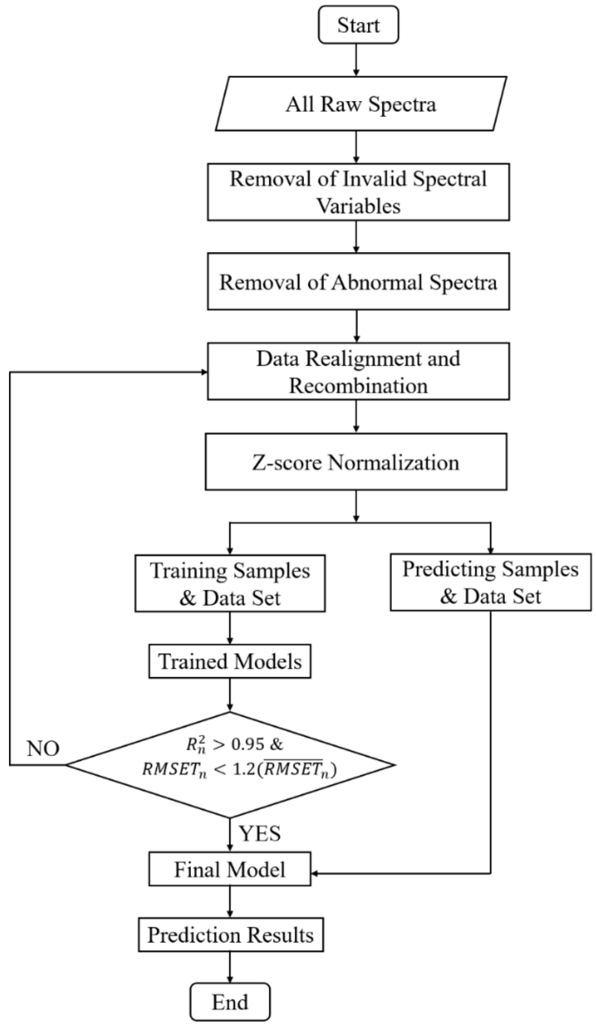

Supplementary Figure 8. Flowchart of raw data treatment and model training and predicting.